ELSEVIER

Journal of Hazardous Materials B137 (2006) 352–358

Journal of Hazardous Materials

www.elsevier.com/locate/jhazmat

Preparation and sorption properties of porous materials from refuse paper and plastic fuel (RPF)

Z. Kadirova [1], Y. Kameshima, A. Nakajima, K. Okada *

Department of Metallurgy and Ceramics Science, Tokyo Institute of Technology, O-okayama, Meguro, Tokyo 152-8552, Japan

Received 16 December 2005; received in revised form 1 February 2006; accepted 10 February 2006
Available online 6 March 2006

Abstract

Porous materials consisting of activated carbon and amorphous $CaO–Al_2O_3–SiO_2$ (CAS) compound were prepared from refuse paper and plastic fuel (RPF), (a mixture of old paper and plastic) by carbonizing and/or activating treatments. Samples formed by chemical activation using K_2CO_3 showed a high specific surface area (S_{BET}) of 1330 m^2/g but a lower ash content due to being washed after activation. By contrast, samples prepared by physical activation using steam showed rather lower S_{BET} (510 m^2/g) due to higher ash contents. The physically activated samples showed much higher uptake properties for Ni^{2+} (a representative heavy metal) and phosphate ions (a representative of a harmful oxyanion) than the chemically activated samples because of the higher content of amorphous CAS in the former samples. By contrast, the chemically activated samples showed higher uptake for methylene blue (MB, a representative organic material) than the physically activated samples because of the higher activated carbon content of higher surface area. Although differences in the sorption properties for Ni^{2+}, phosphate ion and MB were found between the physically and chemically activated samples, both samples show excellent multiple sorption properties for cation–anion combinations and inorganic–organic sorbents.

Keywords: RPF; Activation; Porous material; Multiple sorption; Activated carbon; $CaO–Al_2O_3–SiO_2$

1. Introduction

Increasing industrial production and expansion of human activity has produced increasing amounts of waste matter and the spread of environmental pollution in the world. Although a high percentage of paper is being recycled, large amounts of old paper and paper sludge are still available due to the limitation in the amount already being recycled. Only a part of the waste is reused as raw material for cement but most is burned to paper sludge ash and landfilled.

One of the new approaches for reuse of paper waste is to form refuse paper and plastic fuel (RPF) [1], which is a mixture of old paper and plastic. The mixing ratio of paper and plastic in RPF ranges from 3:7 to 7:3 and the resulting RPF has the following properties; bulk density 0.36–0.45 g/cm^3, carbon content 65–56 mass%, ash content 4.2–6.3 mass% and heat of combustion 30–20 kJ/g. To avoid generation of dioxins by burning the RPF, the plastics used in RPF are restricted to those which do not contain chlorine.

Since paper contains cellulose fibers as its main constituent, activated carbon can be prepared from it [2–4]. Shimada et al. [2] prepared raw material for activated carbon by mixing and hot forming old newspaper with phenol resin, and produced activated carbon by physical activation using steam. These activated carbons had specific surface areas of about 1000 m^2/g and adsorption properties for I_2 (1300 mg/g) and methylene blue (330 mg/g) similar to those of commercial activated carbons. By contrast, we have prepared activated carbon by chemical and physical activation using old paper only [3,4]. The activated carbons prepared by chemical activation using K_2CO_3 had high specific surface areas of about 1700 m^2/g and adsorption properties for water vapor (1000 ml/g) and methylene blue (390 mg/g), rather higher than those of commercial activated carbons. The activated carbons prepared by physical activation using steam maintained the original paper shape though the porous and adsorption properties were lower than those prepared by chemical activation. One of the reasons for the

* Corresponding author. Tel.: +81 3 5734 2524; fax: +81 3 5734 3355.
E-mail address: kokada@ceram.titech.ac.jp (K. Okada).
[1] Present address: Institute of General and Inorganic Chemistry Academy of Sciences, Abdullaev Street 77a, Tashkent 700170, Uzbekistan.

0304-3894/$ – see front matter © 2006 Elsevier B.V. All rights reserved.
doi:10.1016/j.jhazmat.2006.02.008

lower porous properties of the physically activated carbons compared with the chemically activated carbons is a higher ash content, originating from inorganic fillers and coating materials, i.e. kaolinite ($Al_2Si_2O_5(OH)_4$), limestone ($CaCO_3$) and talc ($Mg_3Si_4O_{10}(OH)_2$).

Although paper contains only a small amount of inorganic matter, its content is more concentrated in the paper sludge. Thus, we have prepared an amorphous $CaO–Al_2O_3–SiO_2$ compound by calcining paper sludge at 500–1000 °C [5] because such compounds (e.g. $CaAl_2Si_2O_8$) prepared from solid-state reaction of kaolinite and $CaCO_3$ show good uptake properties for various heavy metal ions [6]. The amorphous $CaO–Al_2O_3–SiO_2$ compound was found to have good uptake properties for not only heavy metal cations but also for eutrophication related ions, i.e. phosphate and ammonium ions [5].

In this paper, porous materials consisting of composites of activated carbon and amorphous $CaO–Al_2O_3–SiO_2$ were prepared by chemical and physical activation using single-step and two-step methods. The multiple sorption properties of the resulting porous materials for Ni^{2+} (a representative heavy metal ion), phosphate ion (a representative harmful oxyanion) and MB (a representative organic material) were investigated.

2. Experimental

2.1. Sample preparation and characterization

The RPF sample was obtained from the Nippon Daishowa Paperboard Co., Tokyo, Japan. The mixing ratio of paper/plastic in the as-received sample was about 5/5 and its physical form was a cylindrical rod several centimeters in size. This was thermally treated by four different methods as shown in Fig. 1: (1) single-step chemical activation (Chem 1), (2) single-step physical activation (Phys 1), (3) two-step chemical activation (Chem 2), and (4) two-step physical activation (Phys 2). The sample was directly activated in the single-step method but in the two-step method it was first carbonized and then activated. The carbonization treatments were performed by heating the RPF at 500 °C for 2 h in flowing dried N_2. Physical activation was performed by heating RPF at 500–900 °C in flowing dried N_2, holding it at temperature for 2 h with the introduction of wet N_2 (20 mol% steam) and cooling in flowing dried N_2. Chemical activation was performed by heating the RPF sample impregnated with K_2CO_3 at 500–900 °C for 2 h in flowing dried N_2. The RPF/K_2CO_3 ratio in the Chem 1 sample was 1/0.627 and the carbonized RPF/K_2CO_3 ratio in the Chem 2 sample was 1/1. In all the experiments, the heating and cooling rates were 10 °C/min and the N_2 flow rate was 500 ml/min. The RPF ash sample was obtained by heating RPF at 1000 °C in air.

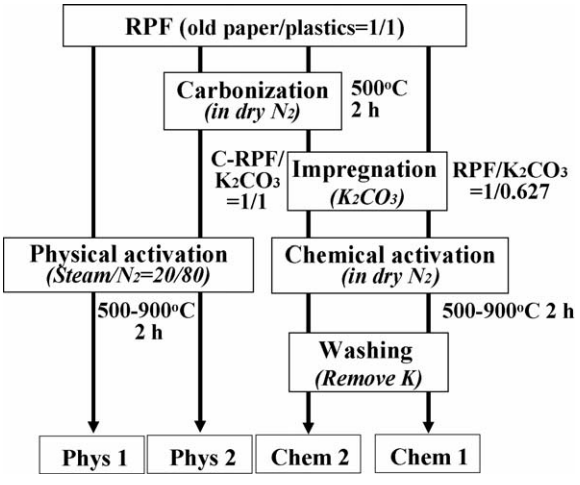

Fig. 1. Experimental flow chart for the preparation of the porous materials.

The chemical composition of the sample was analyzed by X-ray fluorescence (RIX2000, Rigaku, Japan). The crystalline phases in the sample were identified by powder X-ray diffraction (XRD-6100, Shimadzu, Japan) with monochromated Cu Kα radiation. The N_2 adsorption–desorption isotherms of the sample were measured using an automatic gas adsorption instrument (Autosorb-1, Quanta Chrome, USA). The specific surface area (S_{BET}) and pore size distribution were calculated by the BET and BJH methods, respectively.

2.2. Sorption experiments

Sorption of Ni^{2+}, phosphate and MB was determined for the Phys 1 sample prepared at 700 °C (Phys 1 (700)) and Chem 2 sample at 900 °C (Chem 2 (900)) because these showed the maximum S_{BET} values after activation. The experiments were performed under the following conditions; temperature: 25 °C, sample/solution ratio: 0.1 g/50 ml, initial concentration of Ni^{2+} (from $NiCl_2{\cdot}6H_2O$ solution), PO_4^{3-} (from $NH_4H_2PO_4$ solution) and MB (from $C_{16}H_{18}N_3SCl{\cdot}3H_2O$ solution): 0.1–20 mmol/l, reaction time: 24 h. The pH values were measured using a pH meter (HM-20J, TOA DKK, Japan) immediately prior to placing the sample into the solution (initial pH) and after the reaction (final pH). After the sorption experiments, the samples were centrifuged at 8000 rpm for 20 min, washed three times with deionized water and dried at 110 °C overnight. The separated solutions were chemically analyzed for Ni^{2+}, Ca^{2+}, Al^{3+} and silicate ions by ICP-OES (Leeman Labs Inc., USA). The phosphate ion concentration was measured by ion chromatograph (IA-200, DKK TOA, Japan). The MB concentration was measured by absorptiometer (S-2400, Soma Chemical, Japan).

3. Results and discussion

3.1. Characterization of the samples

The average chemical compositions of RPF ash, carbonized and activated (Phys 2 (900) and Chem 2 (900)) samples are listed in Table 1. The main constituents of the RPF ash are SiO_2, CaO and Al_2O_3, related to the major raw materials kaolinite and limestone. The average ash content in the RPF was 4.7 mass%. After carbonization, the ash content increased to about 23 mass%, the accompanying weight losses being mainly due to the decomposition of cellulose ($[C_6H_{10}O_5]_n$) to carbon and to the dehydroxylation of kaolinite. Physical activation caused the ash content to increase with increasing activation temperature. Thus, the ash

Table 1
Chemical compositions of RPF ash, carbonized and activated samples

Sample	C	SiO_2	Al_2O_3	CaO	MgO	Fe_2O_3	TiO_2	K_2O	Na_2O	Cl	SO_3	P_2O_5
RPF ash	–	37.2	16.4	23.9	5.7	0.7	6.3	0.3	6.9	0.1	1.9	0.5
Carbonized	77.5	5.9	3.8	6.7	1.3	0.3	2.4	0.1	1.2	0.2	0.3	0.1
Phys 2 (900)	55.2	12.7	8.4	13.4	2.8	0.6	4.1	0.2	1.8	0.1	0.4	0.3
Chem 2 (900)	71.9	8.5	5.3	6.7	2.3	0.6	3.5	0.8	0	0	0.2	0.1

content of the 900 °C sample reached 45 mass%. By contrast, the ash content in the chemically activated samples showed only a slight change with temperature, being about 28 mass% after treatment at 900 °C. The lower ash contents in the chemically activated carbons are due to the presence of highly water-soluble potassium aluminosilicate thought to be formed by reaction of the inorganic matter with K_2CO_3 during activation, then partly leached away during the washing treatment.

The XRD patterns of the physically (a) and chemically (b) activated samples are shown in Fig. 2. The carbonized sample shows many peaks corresponding to calcite, talc, anatase and rutile as well as a halo corresponding to amorphous carbon. The peaks of kaolinite are not observed in the carbonized sample because it is converted to X-ray amorphous metakaolinite by the carbonization treatment. In the physically activated samples (Phys 2) prepared at 500–900 °C, the peak intensities of calcite weaken then disappear at 700 °C, the decomposition of this phase being accelerated by the humid atmosphere. At 700 °C, the peaks corresponding to talc also disappear and the sample becomes mostly amorphous apart from small amounts of crystalline TiO_2 (anatase and rutile). Above 700 °C, a new phase, gehlenite ($Ca_2Al_2SiO_7$) is formed by partial crystallization of amorphous $CaO–Al_2O_3–SiO_2$ [7]. The XRD patterns of the chemically activated samples (Chem 2) prepared at 700–900 °C are similar, showing a clear peak corresponding to calcite and a halo corresponding to amorphous carbon and amorphous $CaO–Al_2O_3–SiO_2$. In these samples, the higher content of carbonate arising from impregnation by K_2CO_3 may increase the decomposition temperature of calcite above the temperature of 900 °C used for physical activation.

Changes in the specific surface areas (S_{BET}) of the resulting porous materials are shown in Fig. 3 as a function of the activating temperature. The Phys 1 and 2 samples show maximum values of S_{BET} at 700 °C (510 m^2/g) and 850 °C (450 m^2/g), respectively. The S_{BET} values of the Chem 1 sample show somewhat strange behavior with activating temperature, i.e. activation at 700 °C produces a very low S_{BET} value. Apart from this sample, S_{BET} increases with increasing activation temperature to a maximum value of about 520 m^2/g at 1000 °C. By contrast with these results, the S_{BET} values of the Chem 2 sample are higher than 600 m^2/g, the maximum S_{BET} becoming as high as 1300 m^2/g at 900 °C. This S_{BET} value is higher than that of activated carbon prepared from refuse-derived fuel (RDF) prepared from municipal waste [8]. The pore size distribution curves of the Phys 1 (700) and Chem 2 (900) samples are shown in Fig. 4. The pores formed in both samples are mainly micropores (<2 nm) but of different sizes; the pores in sample Chem 2 (900) are about 2 nm while those in sample Phys 1 (700) are <1.2 nm. Thus, the higher S_{BET} value of sample Chem 2 is attributed to its lower ash content and pore size. These results are similar to those found for physically and chemically activated carbons prepared from old paper [3] but the pore size obtained for sample Chem 2 (900) is larger than that from old paper. This may be due to differences in the raw materials with and without plastic.

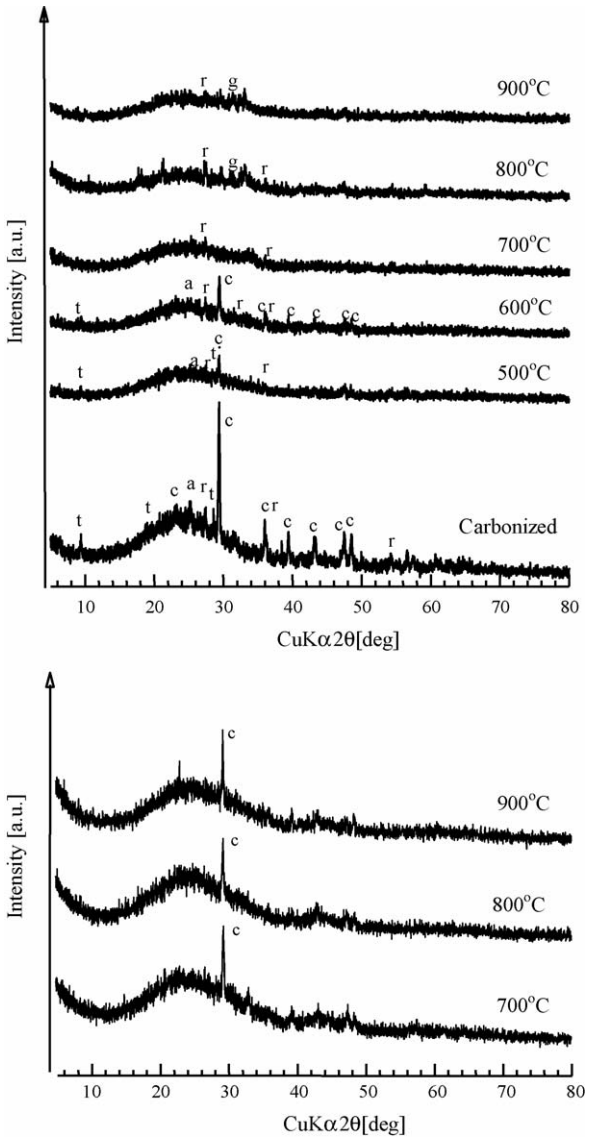

Fig. 2. XRD patterns of the carbonized sample and Phys 2 samples activated at various temperatures. The labels on the XRD patterns are: a, anatase (TiO_2); c, calcite ($CaCO_3$); g, gehlenite ($Ca_2Al_2SiO_7$); t, talc ($Mg_3Si_4O_{10}(OH)_2$).

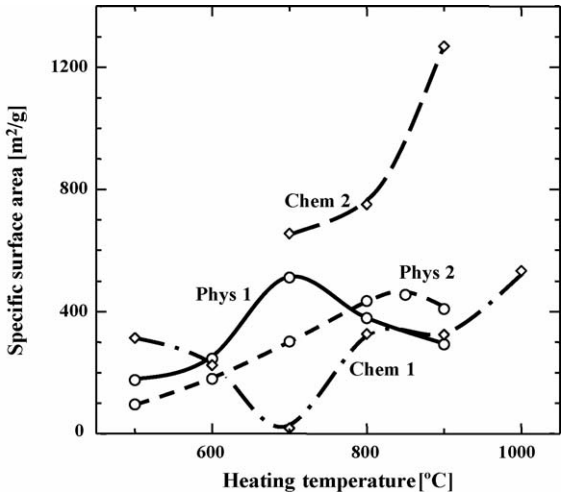

Fig. 3. Change of specific surface areas of the four different activated samples as a function of activating temperature.

3.2. Sorption properties

The sorption isotherms for Ni^{2+}, phosphate and methylene blue (MB) of the Phys 1 (700) and Chem 2 (900) samples were determined as examples of the sorption ability of these materials for heavy metal ions, harmful oxyanions and organic dyes. The Ni^{2+}, phosphate and MB sorption isotherms are shown in Fig. 5. All of them show steep increase in the region of low equilibrium concentration but stable at higher concentrations. These isotherm data were fitted by the Langmuir and Freundlich equations

$$\frac{C_e}{Q_e} = \left(\frac{1}{Q_0}\right) C_e + \left(\frac{1}{Q_0 b}\right) \quad (1)$$

$$Q_e = K_F C_e^{1/n} \quad (2)$$

where C_e is the equilibrium concentration (mmol/l), Q_e the amount sorbed at equilibrium (mmol/g), Q_0 the sorption capacity (mmol/g), and b is the Langmuir constant (l/mol), and K_F (mmol/g) and n are the Freundlich constants. The free energy of sorption (ΔG; kJ/mol) can be calculated from the parameter b

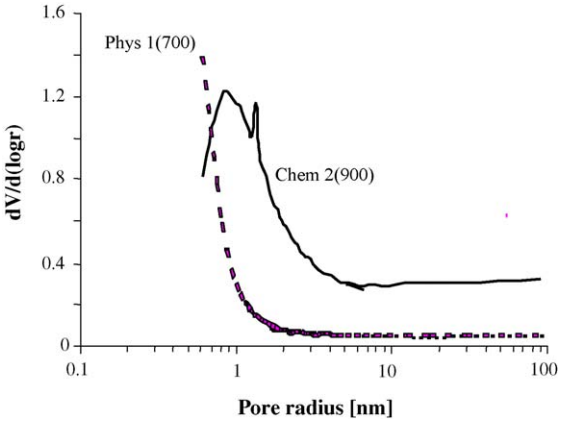

Fig. 4. Pore size distributions of the Phys 1 (700) and Chem 2 (900) samples.

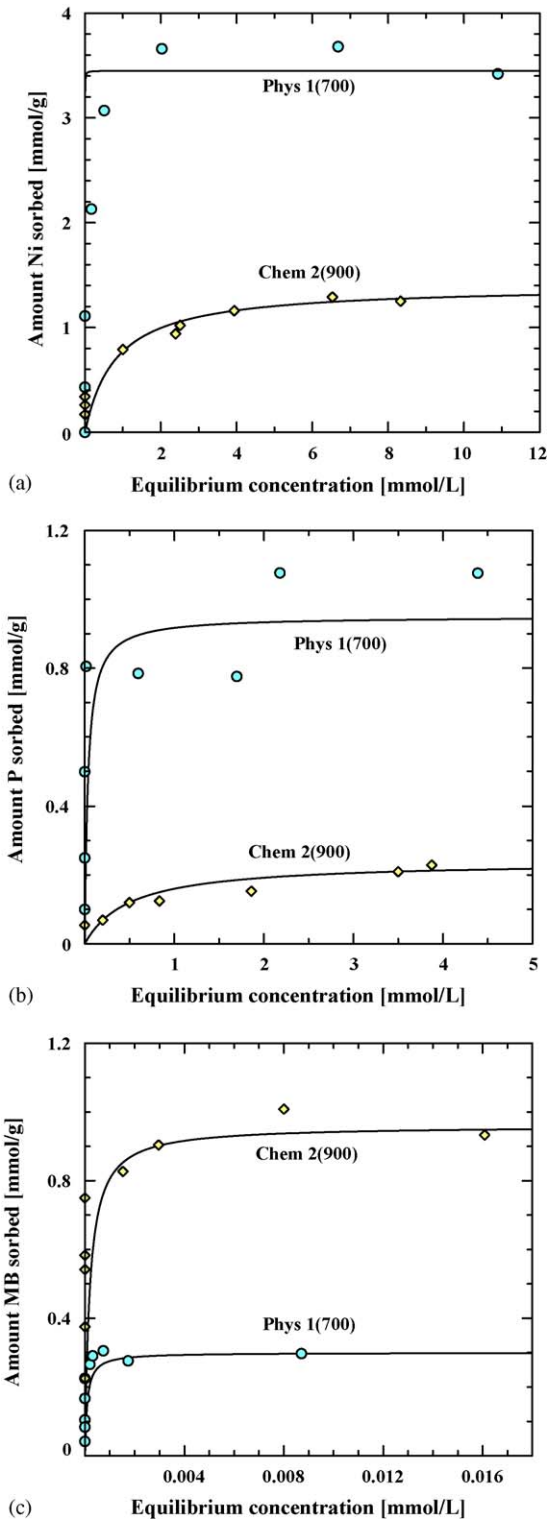

Fig. 5. Ni^{2+} (a), phosphate (b), and methylene blue (c) sorption isotherms of the Phys 1 (700) and Chem 2 (900) samples.

using the following equation:

$$\Delta G = -RT \ln(b) \quad (3)$$

where R is the gas constant (8.314 kJ/mol K) and T is the temperature (K).

Table 2
Sorption properties for Ni^{2+}, phosphate and methylene blue (MB) by the Phys 1 (700) and Chem 2 (900)

Adsorbate	Sample	Langmuir parameter				Freundlich parameter		
		Q_0 (mmol/g)	b (l/mmol)	R^2	ΔG (kJ/mol)	K_F (mmol/g)	n	R^2
Ni^{2+}	Phys 1 (700)	3.45	2900	0.9986	−36.9	2.93	10.9	0.6403
	Chem 2 (900)	1.40	1.23	0.9943	−17.6	0.81	4.28	0.8789
Phosphate	Phys 1 (700)	0.95	27.8	0.9591	−25.4	0.87	38.3	0.1469
	Chem 2 (900)	0.24	2.00	0.9539	−18.8	0.13	2.53	0.961
MB	Phys 1 (700)	0.30	11160	0.9976	−40.2	0.32	62.9	0.8839
	Chem 2 (900)	0.96	5230	0.9970	−38.3	2.07	6.20	0.9964

The sorption capacities (Q_0), Langmuir constants (b) and free energies of sorption (ΔG) of Ni^{2+}, phosphate and MB for the Phys 1 (700) and Chem 2 (900) samples are listed in Table 2. Judged by the resulting correlation coefficients (R^2), the Langmuir equation gives a better fit for all the samples than the Freundlich equation. The Q_0 values of Ni^{2+} and phosphate are 2–4 times higher in sample Phys 1 (700) than in sample Chem 2 (900) though the S_{BET} value of sample Phys 1 (700) is less than half that of sample Chem 2 (900). Thus, the sorption of Ni^{2+} and phosphate is found to be associated more with the amorphous $CaO–Al_2O_3–SiO_2$ phase and less with the activated carbon. As reported elsewhere [5–7], sorption mechanisms of Ni^{2+} by amorphous $CaO–Al_2O_3–SiO_2$ phase are mainly attributed to ion substitution for Ca^{2+} while those of phosphate are attributed to adsorption to aluminol groups and precipitation as calcium phosphate phase. In the present samples, ion substitution mechanism for Ni^{2+} sorption is confirmed by almost coincidence in the amounts of sorbed Ni^{2+} and released Ca^{2+}. Formation of calcium phosphate is indicated by the decrease of Ca^{2+} concentration with higher initial phosphate concentration in the phosphate sorption experiments. On the other hand, the Q_0 value for MB is about three times higher in sample Chem 2 (900) than in sample Phys 1 (700). This result is attributed to the higher S_{BET} value and larger pore size of the activated carbon in sample Chem 2 (900). Thus, sorption of MB by activated carbon is attributed to adsorption mechanism [9]. The ΔG values for Ni^{2+}, phosphate and MB sorption by both samples are negative (Table 2). All the sorption reactions are thus thought to occur spontaneously. Although there are differences in the sorption capacities for Ni^{2+}, phosphate and MB by the two samples, they show good multifunctional sorption ability for cations and anions because of the co-presence of activated carbon and amorphous $CaO–Al_2O_3–SiO_2$, the latter phase showing multifunctional sorption properties [5].

In the sorption experiments, final pH shows considerable changes with chaining of initial concentrations of Ni^{2+} and phosphate in both samples. In the Ni^{2+} sorption experiments, the final pH values in Phys 1 (700) sample changed largely from about 11 to 4 with higher equilibrium concentration C_e while those in Chem 2 (900) sample changed only from about 9.5 to 7. Higher the final pH values in lower C_e conditions are attributed to the excess dissolution of Ca^{2+} from amorphous $CaO–Al_2O_3–SiO_2$ phase while lower the final pH values in higher C_e conditions are corresponded to the excess amount of adsorbate after the sorption experiments. The changes of the final pH are apparently larger in Phys 1 (700) than Chem 2 (900) samples. This may be due to the residual surface alkali ions in the Chem 2 (900) sample. The concentrations of silicate anions are mostly 0.3–0.6 mmol/l and almost stable in all the sorption experiments. This may suggest that the silicate anions are saturated state in their solutions. By contrast, Al^{3+} was not detected in most of the samples but the concentrations increased largely when the final pH of the samples become <5 and ≥10.5.

Since the molecular size of MB is much larger than Ni^{2+} and the phosphate ion, its sorption rate in the Phys 1 (700) and Chem 2 (900) samples was investigated. Fig. 6 shows the amount of MB sorption by the two samples as a function of reaction time. The sorption is found to occur within a short time in the both samples. Although many models have been proposed to simulate the sorption kinetics [7,10–12], the present data were analyzed using a pseudo first order Lagergren equation (Eq. (4)), second order equation (Eq. (5)), and intraparticle diffusion equation (Eq. (6))

$$\log(Q_e - Q(t)) = -\left(\frac{k_1}{2.303}\right) t + \log Q_e \quad (4)$$

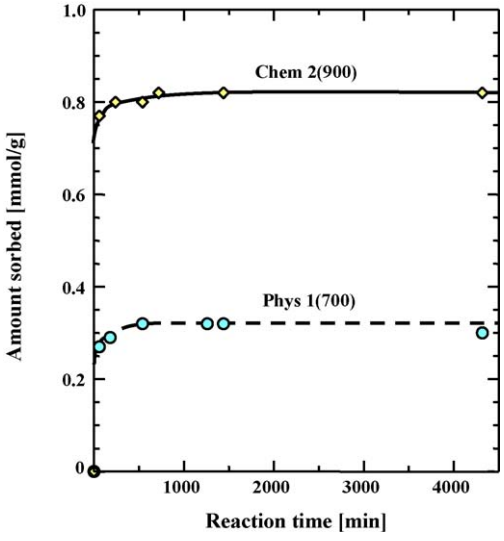

Fig. 6. Changes in the amount of MB sorption by the Phys 1 (700) and Chem 2 (900) samples as a function of reaction time.

Table 3
Kinetic data on sorption of MB by the Phys 1 (700) and Chem 2 (900) samples

Model	Parameter	Sample	
		Phys 1 (700)	Chem 2 (900)
–	Q_e^{obs} (mmol/g)	0.33	0.83
First order model	k_1 (l/min)	3.04×10^{-3}	2.91×10^{-3}
	Q_e^{calc} (mmol/g)	0.07	0.06
	R^2	0.9979	0.7333
Second order model	k_2 (g/mmol min)	0.15	0.13
	Q_e^{calc} (mmol/g)	0.33	0.83
	R^2	0.9998	0.9999
Intraparticle diffusion	k_3 (mmol/min$^{1/2}$ g)	1.72×10^{-3}	1.72×10^{-3}
	$Q(0)$ (mmol/g)	0.27	0.77
	R^2	0.9188	0.7965

$$\frac{t}{Q(t)} = \frac{t}{Q_e} + \frac{1}{k_2 Q_e^2} \quad (5)$$

$$Q(t) = k_3 t^{1/2} + Q(0) \quad (6)$$

where Q_e, $Q(t)$ and $Q(0)$ (mmol/g) are the amounts of sorption at equilibrium, at time t and at time = 0 (min), respectively, and k_1 (l/min), k_2 (g/mmol min) and k_3 (mmol/min$^{1/2}$ g) are the first order sorption, second order sorption and intraparticle diffusion rates, respectively. The calculated data are listed in Table 3. The sorption rates of the two samples calculated are very similar for the three models (k_1, k_2 and k_3). Although the two samples have apparently different sorption capacities for Ni^{2+}, phosphate and MB, their sorption rates are very similar. The MB sorption rates of both samples show better correlation with the second order model than with the other two models. Thus, the calculated Q_e values are very close to the observed values from the second order model but are distinctly different from the first order model. It is therefore thought that the second order model is plausible for the MB sorption kinetics. The resulting sorption rates are rather lower than those reported for other sorbents [9,13–15]. This may be attributed to the small pore sizes of the present samples relative to the large and elongated MB molecules.

4. Conclusion

Porous materials consisting of activated carbon and amorphous $CaO–Al_2O_3–SiO_2$ were prepared by physical and chemical activation of refuse paper and plastic fuel (RPF). The following results were obtained:

(1) The ash content in the samples was higher in the physically activated sample (≤45 mass%) than in the chemically activated sample (≤28 mass%), in which it was decreased by the washing treatment.
(2) The maximum specific surface area obtained was higher in the sample chemically activated by a two-step process (about 1300 m^2/g) than in the physically activated samples (about 500 m^2/g).
(3) Both samples showed multisorption properties for Ni^{2+} (representative of a heavy metal), phosphate (representative of a harmful oxyanion) and MB (representative of an organic dye).
(4) The physically activated sample showed higher sorption capacity for Ni^{2+} and phosphate while the chemically activated sample showed a higher sorption capacity for MB.
(5) The MB sorption rates of the two samples are almost identical and relatively low due to the small pore size compared with the large MB molecule.

Acknowledgements

ZK thanks UNESCO/MEXT, Japan for the award of a research fellowship. The authors are grateful to Professor K.J.D. MacKenzie of Victoria University of Wellington for critical reading and editing of the manuscript. The authors are also thank to Nippon Daishowa Paperboard Company for supplying the RPF sample.

References

[1] R. Ohe, et al. (Eds.), Handbook of Old Paper 2002, Paper Recycling Promotion Center, Tokyo, 2002.
[2] M. Shimada, H. Hamabe, T. Ida, K. Kawarada, T. Okayama, The properties of activated carbon made from waste newsprint paper, J. Porous Mater. 6 (1999) 191–196.
[3] K. Okada, N. Yamamoto, Y. Kameshima, A. Yasumori, Porous properties of activated carbons from waste newspaper prepared by chemical and physical activation, J. Colloid Interface Sci. 262 (2003) 179–193.
[4] K. Okada, N. Yamamoto, Y. Kameshima, A. Yasumori, Adsorption properties of activated carbons from waste newspaper prepared by chemical and physical activation, J. Colloid Interface Sci. 262 (2003) 194–199.
[5] V.K. Jha, Y. Kameshima, A. Nakajima, K. Okada, K.J.D. MacKenzie, Multifunctional uptake behaviour of materials prepared by calcining waste paper sludge, J. Environ. Sci. Health A, in press.
[6] K. Okada, N. Watanabe, V.K. Jha, Y. Kameshima, A. Yasumori, K.J.D. MacKenzie, Uptake of various cations by amorphous $CaAl_2Si_2O_8$ prepared by solid-state reaction of kaolinite with $CaCO_3$, J. Mater. Chem. 13 (2003) 550–556.
[7] V.K. Jha, Y. Kameshima, K. Okada, K.J.D. MacKenzie, Ni^{2+} uptake by amorphous and crystalline $CaAl_2SiO_7$ synthesized by solid-state reaction of kaolinite, Sep. Purif. Technol. 40 (2004) 209–215.
[8] S. Nagano, H. Tamon, T. Adzumi, K. Nakagawa, T. Suzuki, Activated carbon from municipal waste, Carbon 38 (2000) 915–920.

[9] N. Kannan, M.M. Sundaram, Kinetics and mechanism of removal of methylene blue by adsorption on various carbons—a comparative study, Dyes Pigments 51 (2001) 25–40.
[10] Y.S. Ho, G. McKay, Comparative sorption kinetic studies of dye and aromatic compounds onto fly ash, J. Environ. Sci. Health A 34 (1999) 1179–1204.
[11] S. Kumar, S.N. Upadhaya, Y.D. Upadhaya, Removal of phenols by adsorption on fly ash, J. Chem. Technol. Biotechnol. 37 (1987) 281–290.
[12] F.C. Wu, R.L. Tseng, C.C. Hu, Comparisons of pore properties and adsorption performance of KOH-activated and steam-activated carbons, Micropor. Mesopor. Mater. 80 (2005) 95–106.
[13] W.T. Tsai, K.J. Hsien, J.M. Yang, Silica adsorbent prepared from spent diatomaceous earth and its application to removal of dye from aqueous solution, J. Colloid Interface Sci. 275 (2004) 428–433.
[14] R.S. Juang, F.C. Wu, R.L. Tseng, Mechanism of adsorption of dyes and phenols from water using activated carbons prepared from plum kernels, J. Colloid Interface Sci. 227 (2000) 437–444.
[15] A. Sharma, K.G. Bhattacharyya, Azadirachta indica (Neem) leaf powder as a biosorbent for removal of Cd(II) from aqueous medium, J. Hazard. Mater. 125 (2005) 102–112.